A Multiscale Analysis Model Applied to Natural Surfaces

Frédéric FALZON Gérard GIRAUDON Marc BERTHOD

INRIA, BP.93, F-06902 SOPHIA ANTIPOLIS Cedex

Abstract

Multiscale Analysis of surfaces allows a hierarchical representation of their composing features. To represent a surface at a given scale, structures that are insignificant at that scale have to be eliminated. A typical example for this approach is cartography. However, the aims of cartographers reach beyond simply gradually eliminating the structures; in the majority of cases, the nature of geomorphological structures which compose the surface have to be preserved across all scales. Thus a global smoothing of the surface is not suitable to solve the present problem, since that would cause inevitably morphological modifications of certain important structures. In fact, the points to be preserved across scale variations are to be chosen interactively by the user. In this paper we present a surface model which allows us to perform a Multiscale Analysis which takes the importance of local structures into consideration i.e. structures which are inherent to the relief morphology. From that discrete model we extract a context-dependent Multiscale Analysis Operator which can be isotropic or anisotropic and can be expressed in different forms.

1 Introduction

This paper is devoted to surface reconstruction analysis for DEM (Digital Elevation Model) cartography applications, and especially deals with multiscale analysis of DEM. A surface model is analyzed as a way to better understand the behaviour of geomorphologic structures in scale-space, and this with the aim to build automatically terrain maps at different resolutions.

In the surface reconstruction domain, numerous works have been published by the researchers of the computer vision community, like [13, 5, 3, 30, 31] and more recently [29, 28].

Most of the approaches use variational formulations often based on generalized splines models and surface representation in the form $z = f(x, y)$ (see the review of methods proposed in [27, 11, 4]). The problem is then to maximize the surface smoothness in conjunction with an error minimization between the model and the data. The discrete optimization is realized iteratively on rectangular grid. Some authors [29, 28] have shown that these approaches introduce drawbacks concerning stability and uniqueness of the solution. Schumaker [27] has proposed to divide the reconstruction in two phases. The first phase consists of a polynomial approximation from a coarse sampling of the data to construct a surface patch. The second phase consists of a refinement to obtain continuity and finer details. [28] uses this scheme with weighted splines and [30] implements a like-scheme to solve his variational problem (constraints on $\rho(x, y)$ and $\tau(x, y)$ pp 421). Another development has been realized recently by [31] and consists of an adaptive network model which discretizes a thin plate surface model. The final solution is an irregular lattice where the node concentration reflects local surface discontinuities. Before giving mathematical aspects, we present the scheme generally used by cartographers for building multiple resolution terrain maps.

(1) Choice of sampling points : From a fine sampling of the surface , choice of reference points to be represented at coarse scales e.g. 1/10000 $\rightarrow$ 1/50000. These points are vertices, ridge lines, stream networks etc... . They have to represent relevant information at a given scale. Therefore, information considered irrelevant at this scale, has to be discarded, while spatial localisation and altimetric values of important structures are preserved. These structures result from a complex visual interpretation which includes an important number of parameters and yields an irregular sampling network (in fact, instead of sampled surfaces, cartographers uses isolevel curves representations).

(2) Interpolation : Piecewise interpolation with nodes as chosen in step (1). Bicubic spline interpolation is frequently used.

This application is strongly governed by human geomorphological interpretation of surfaces. In the Schumaker's and Sinha's strategies, nodes could not be located where the morpholgy has to be preserved at a given scale. To avoid these problems nodes can be put in accordance to detail concentrations with an adaptive node distribution [31]. But the number of nodes is given a priori, independently of geomorphological analysis and this scheme leads to an inverse methodology which is used by cartographers. In order to realize relevant information extraction, we propose a two phases approach where the same network with regular node distribution is used at each phase; this constitutes an alternative to splines. Our analysis-

0-8186-2840-5/92 $03.00 © 1992 IEEE

reconstruction scheme which allows us to represent a surface at a given scale is as follows :

- **Phase 1** : **(1) Multiple Scale representation** of the surface, **(2) Detection and localization** of surface features
- **Phase 2** : **(3) Refinement** of the data obtained at stage (2): Focusing on zones where details are numerous and redo step (1) and (2) until no new zone is detected, **(4) Reconstruction** of the surface from sparse data obtained in (3).

The reconstruction problem is an ill-posed problem [25, 34], therefore our goal is to obtain the "best" reconstruction in the sense of the criteria given in stage (2). The purpose of this paper is to propose a well suited surface model to a regular representation (stages 1-2) and to an irregular representation (stages 3-4). We will focus upon the ability of this model to adapt itself to multiple situations invoked in our scheme, and we give results in the framework of surface reconstruction (other results are given in [9]). To include this model in a resolution change algorithm, we will concentrate on its ability to take into account external knowledge to modify its local behaviour and to integrate constraints. In section 2 we review multiscale and multiresolution analysis and we give the conditions necessary for well suited scale changes in the 2D case. In section 3 we study a model which leads to a 1D discrete scaled operator. We give its properties and a definition which characterizes its aptitude to create scale-space in an isotropic case. In section 4 we give the 2D version of this model. In section 5 we give three filters which are frequency analoguous to the 1D-isotropic, 2D-isotropic and 2D-anisotropic scaled operators. In section 6 we study the reconstruction problem applied to DEM. We restrict our study to the case where some important points are fixed and are used for the reconstruction. We do not study the subsampling problem (the resolution changes). Finally, we conclude with the ability of this model to be inserted in a global analysis-reconstruction algorithm.

2 Multiscale Analysis - Multiresolution Analysis (MSA-MRA) and associated models

2.1 MSA - MRA a review

Computer vision community has been interested in problems of MSA and MRA since David Marr's works on edge detection.

Why use MSA in computer vision ? Essentially to detect macro structures corrupted by noise or non significant details, at a given scale. But the major problem is to connect the notion of scale with the regularity degree of a signal or with the density of details in it. Until now this problem is not well solved, because it is very difficult to characterize details. The only thing that we can say is that details are high frequency components, and the best way to reduce their effect is to make a low pass filtering or more generally a band pass filtering with variable bandwidth. Here the bandwidth plays the role of a scale. In the cartography framework , a scale change induces automatically a resolution change. Our definition of scale and resolution is slightly different. We define a resolution change as a subsampling of the image followed by a smoothing (the support of the image at lower resolutions is smaller than the original one). A scale change is defined as the smoothing of the image without subsampling. This means that, according to the Shannon theorem, scale change is a redundant resolution change. The most famous application of the scale notion is due to Marr and Hildreth [22] who stated that : *An image is characterized by its local intensity variations at each scale.* With this principle they have proposed an image analysis strategy which consists of the convolution of the image with the laplacian of the Gaussian, the standard deviation playing the role of a scale selection. Recently it has been shown that this type of analysis can be associated with time-scale technics like wavelets (the second derivative of the gaussian is called Marr wavelet) [12]. Within the scope of MRA one can cite the pyramidal representations of [6, 20, 1].

2.2 Multiscale Analysis from Witkin and Koenderink

Witkin [32] first proposes a quantitative method which leads to contour representation in scale-space. Later Koenderink [16] justified the use of a Gaussian kernel and demonstrated that it is the only kernel well suited for MSA. Koenderink gives two definitions which have to be respected to make a "good" MSA

Definition 2.1 *Any feature present at a coarse scale is required to possess a cause at a finer scale although the reverse need not be true.*

Definition 2.2 *The smoothing is required to be space invariant.*

The first definition prevents the model from generating spurious details when the scale is diminished (causality principle), while the second leads to an isotropic and homogeneous smoothing. With some background in physical mathematics, it can be seen that these two definitions are verified by a diffusion equation such as the heat equation. This allows us to write the equations of the model which leads to MSA : Let $\tilde{P}(x,y)$ the original image and $P(x,y,t)$ the image at scale t . $P(x,y,t)$ is the solution of the problem

$$P_t(x,y,t) = \zeta\,(P_{xx}(x,y,t) + P_{yy}(x,y,t)) \qquad (1)$$

where $P(x,y,0) = \tilde{P}(x,y)$ is the initial condition and ζ is the diffusion coefficient.

In this problem we treat an infinite domain where the heat spreads out according to a law given by its solution, which has the following form :

$$P(x,y,t) = \int\int_{\mathbb{R}^2} \tilde{P}(x-\tilde{x}, y-\tilde{y})\, G(\tilde{x},\tilde{y},t)\, d\tilde{x}\, d\tilde{y} \quad (2)$$

with

$$G(x,y,t) = \frac{1}{2\zeta\sqrt{\pi t}} \exp \frac{-(x^2+y^2)}{4\zeta^2 t} \qquad (3)$$

As we can see, solving equation (1), with initial conditions, leads to the evaluation of a convolution integral (2) with a Gaussian kernel (with standard deviation $\sigma = \zeta\sqrt{2t}$).

We can also write a geometric heat equation, in which the curvature is explicitly the second member i.e. the curvature is scaled (see [23]).

According to these considerations, [2] (in 1D) and [33] (in 2D), have mathematically proved the uniqueness of the solution obtained with a Gaussian kernel and its ability to verify the two Koenderink's principles (some precisions about zero-crossings behaviour of the filtered image can also be found in [33]).

Now if we consider the problem of a spatially bounded domain, we can give a new formulation which includes boundary conditions (but generally, in computer vision problems, we prefer models in which we do not have to worry about boundary conditions). The boundary conditions can be formulated in two forms and lead to two different problems called *Neumann problem* and *Dirichlet problem* ([15, 10, 7]) :

- *Neumann Problem :*

$$P_t(x,y,t) = P_{xx}(x,y,t) + P_{yy}(x,y,t)$$

$$P(x,y,0) = \tilde{P}(x,y) \qquad (x,y) \in \Omega$$

$$\frac{\partial P(x,y,t)}{\partial n} = g(x,y) \qquad (x,y) \in \partial\Omega$$

With Ω the domain delimited by the image and $\partial\Omega$ its boundary. $\frac{\partial P}{\partial n}$ is the gradient in the direction given by the normal at the domain.

- *Dirichlet Problem :*

$$P_t(x,y,t) = P_{xx}(x,y,t) + P_{yy}(x,y,t)$$

$$P(x,y,0) = \tilde{P}(x,y) \qquad (x,y) \in \Omega$$

$$P(x,y,t) = \hat{P}(x,y) \qquad (x,y) \in \partial\Omega$$

($\hat{P}(x,y)$ *is a bidimensional function which lays down on the boundary and* $\tilde{P}(x,y)$ *is an initial condition*).

The difference between these two schemes is that in the Dirichlet problem, we impose a boundary function and in the Neumann problem we impose a condition on the derivative of the solution on the boundary e.g. if we put $g(x,y) = 0$ we have a mean (or mass) conservation across the time.

However the studies made in [2] and [33], were realized in continuous space and time. Lindeberg [17] has studied the discrete case and has proved that the only manner to implement discrete MSA is to discretize the diffusion equation. He also demonstrated that if we discretize the convolution integral (so the Gaussian kernel) we do not respect the Koenderink's principles (this problem is not emphasized in the two previous papers). In the framework of anisotropic filtering [24] proves too that properties exhibited in the continuous case do not hold in the discrete case.

From these condiderations, we will describe, in the next section, a discrete evolution surface model obtained by mere topological considerations (neighbourhoods). Due to the fact that we have to introduce conditions in some points, it will be necessary for the model to take into account particular conditions, such as particularly boundary conditions. From this model we obtain an MSA operator which has the same properties that we shall have in the case of discrete heat kernels with Neumann boundary conditions. We show that MSA could be mathematically expressed by a contraction (in the topological sense). At first we study a 1D model based on a connectionist approach and described by a well known analog network. Then we will show that it is easy to extend it in 2D and we give an example of DEM reconstruction.

3 A discrete model of surface evolution - MSA operator

Models based on connectionist approaches are well known in neural computation, and the natural way to represent relation between pixels is given in fig (1). The goal is to obtain "polymorphic" relations between nodes, directed by the context in which they are placed. And this to perform local modifications of pixels interactions. In this way, node interactions

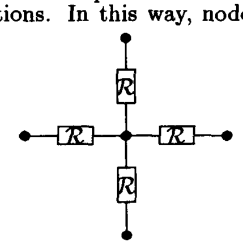

Figure 1: *Relation modeling : Each point is connected with its neighbour by a device* $\mathcal{R}$.

can individually be adapted by use of external measures such as, for example, local differential measures of the surface. To implement this model an analog network analogy seems to be well adapted. Then each pixel (node) is connected to its neighbour by a device such as a resistor, if we want linear inter-pixel relation, or by another device if we want non-linear inter-pixel relation. Analog networks have been extensively used in many domains such as regularization theory [25], reflectance modelisation [14](pp.196-197), image smoothing and segmentation [18] and for the simulation of a biological retina [19].

3.1 Notations

Let Ω be a set of nodes p_i distributed on a line, we note

$\mathcal{V}(p_i) = \{p_k \in \Omega \,, \, |i-k| = 1\}$, the neighbourhood of the node p_i ;

$int\Omega = \{p_i \in \Omega, \, \mathcal{V}(p_i) \subset \Omega\}$, the interior of the set Ω ;

$\partial\Omega = \Omega - int\Omega$, the boundary of Ω ;

and to deal with electrical analogy we note

α_j^i: The device connected between two nodes i and j ($\alpha_j^i \in \mathbb{R}^+$);

V_i : The difference of potential between the node i of the network and a reference;

I_i : The intensity injected in a node . This intensity appears when we apply a difference of potential $\tilde{V}_i$ (network power supply);

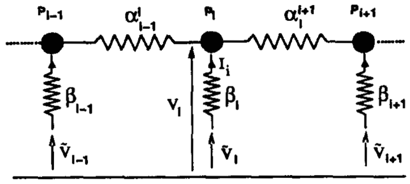

Figure 2: *1D network structure*

3.2 1D model and associated MSA operator

In this study we assume that $\beta = 1$. The network equilibrium equation obtained by Kirchhoff's laws in matrix form (with N the number of nodes i.e. $Card\,\Omega = N$) is given by

$$\tilde{V} = \mathbf{\Gamma}_\alpha \, V \tag{4}$$

$$\mathbf{\Gamma}_\alpha \in \mathbb{R}^{N \times N} \,, V \in \mathbb{R}^N \,, \, \tilde{V} \in \mathbb{R}^N$$

with

$$\mathbf{\Gamma}_\alpha = \begin{pmatrix} \mathcal{Y}_1 & \frac{-1}{\alpha_1^2} & 0 & \dots & \dots\dots & \dots\dots & 0 \\ \frac{-1}{\alpha_2^1} & \mathcal{Y}_2 & \frac{-1}{\alpha_2^3} & 0 & \dots\dots & \dots\dots & 0 \\ \dots & \dots\dots & \dots & \dots & \dots\dots & \dots\dots & \dots \\ 0 & \dots 0 & \frac{-1}{\alpha_i^{i-1}} & \mathcal{Y}_i & \frac{-1}{\alpha_i^{i+1}} \; 0 & \dots & 0 \\ \dots & \dots\dots & \dots & \dots & \dots\dots & \dots\dots & \dots \\ 0 & \dots\dots & \dots & \dots\dots & 0 & \frac{-1}{\alpha_N^{N-1}} & \mathcal{Y}_N \end{pmatrix}$$

and $\mathcal{Y}_i = 1 + \sum_{k \in \mathcal{V}(p_i)} \frac{1}{\alpha_i^k}$

The resolution of the linear system (4) will give us the vector V knowing the vector of supply voltages $\tilde{V}$.

If we make the assumption : $\alpha_i^k = \alpha_k^i = \alpha = Const \quad \forall\, i, k \in int(\Omega)$, the value of the voltage of a node is given by

$$V_i = \frac{\tilde{V}_i}{1 + \sum_{k \in \mathcal{V}(p_i)} \frac{1}{\alpha}} + \frac{\sum_{k \in \mathcal{V}(p_i)} V_k}{\alpha(1 + \sum_{k \in \mathcal{V}(p_i)} \frac{1}{\alpha})} \tag{5}$$

Henceforth we consider V_i as a discrete function of the index i and we give a geometrical interpretation of this model writing (5) in the following form

$$V_i = \tilde{V}_i + \alpha^{-1}\,(V_{i-1} - 2V_i + V_{i+1}) = \tilde{V}_i + \alpha^{-1}\,\mathcal{K}_{loc} \tag{6}$$

$\mathcal{K}_{loc}$ gives information on the curvature sign, then α being positive, concave parts (negative curvatures) tend to move downwards and the convex parts (positive curvatures) tend to move upwards when α decreases. It is now clear that α may be understood as a scale or as a smoothness control parameter, and $\mathbf{\Gamma}_\alpha^{-1}$ as the MSA operator. The effect induced by this operator is a contraction because it decreases the norm of all vector it is applied to (see [9]). According to the previous equations it follows that all the solutions indexed by the parameter α are staying between the initial function and its mean.

$$\lim_{\alpha \to +\infty} V_i = \tilde{V}_i \tag{7}$$

$$\lim_{\alpha \to 0} V_i = \frac{V_{i-1} + V_{i+1}}{2} = \overline{\tilde{V}_i} \tag{8}$$

($\overline{\tilde{V}_i}$ is the mean value of $\tilde{V}_i$).

We can now summarize some properties induced by the MSA operator that we note for convenience $\mathbf{\Psi}_\alpha = \mathbf{\Gamma}_\alpha^{-1}$:

(1) If $\alpha \in \mathbb{R}^+$ is a scale, then for $\alpha_2 < \alpha_1$ the curvature in each point of the curve described at the scale α_2 is lower than the curvature of the curve described at the scale α_1 . **(2)** The function described at the lowest scale is the mean of the original one. And trivially, the function described at the highest scale is the function itself (by equations (7) and (8)). **(3)** The mean is preserved across the scales thus constant functions are not modified by scale changes. **(4)** Due to the dissipative effect of the model, if the initial condition includes a discontinuity, the scaled solutions will always be continuous.

Finally we can mathematically express the hierarchy obtained using the operator $\mathbf{\Psi}_\alpha$ by the following definition

Definition 3.1 *Let V be a discrete bounded function defined on a discrete normed space E where the norm is defined by $\| V \| = \sup_i |V_i|$. We can define a family of functions belonging to E and indexed by a scale j, such as $V^j = \mathbf{\Psi}_j \, V$. If we take the mean as a reference then the hierarchy is expressed by : $0 < \ldots < \| V^j \| < \| V^{j-1} \| < \ldots < \| \tilde{V} \|$*

Some examples of one dimensional MSA can be seen in [9].

Remark 1 : If in (4) we take $\alpha = \zeta^{-1} \frac{\Delta_x^2}{\Delta_t}$ (Δ_t a time discretization step and Δ_x a space discretization step), then (4) is the implicit discretization of the heat equation with Neumann boundary conditions (see [9]).

Remark 2 : We can show ([9]) that the equation of our model is closely related to a Markov chain because the matrix Ψ_α is stochastic i.e. $0 \leq \Psi_\alpha(i,j) \leq 1 \quad , \sum_j \Psi_\alpha(i,j) = 1, \quad \forall (i,j) \in N \times N$ and $\alpha \in \mathbb{R}^+$. Then Ψ_α is the transition probability matrix of a Markov chain. Another stochastic formulation have been used in [18] in the framework of image restoration and in ([21] pp.114).

3.3 Upper value of α

It is interesting to know the value of α which leaves the MSA numerically inactive (i.e. the function to be smoothened is left unchanged when α take a certain value). To obtain this value we take an entropy measure of the smoothened function. Suppose that a scale change is made from the normalized initial function $V = \Psi_\alpha \frac{\tilde{V}}{\|\tilde{V}\|}$, the entropy is given by $H_\alpha = -\sum_i V_i \log V_i$, $V_i \geq 0$. The upper value of the parameter α is obtained by $\alpha_{max} = \{\alpha : \frac{H_\alpha}{\|H_\alpha\|} \simeq 1\}$. It can be shown that for a large class of functions $\alpha_{max} \approx 2.0$ is obtained; then it is sufficient to take $\alpha \in]0 \ldots 2.0]$ to make the MSA.

4 2D model

The extension of the previous model to the 2D case is straightforward, by considering appropriate neighbourhoods (4, 8 connectivity and so on). Thus in the case of 4-connectivity and 8-connectivity, we note the associated operators Γ^4_α and Γ^8_α. These operators are banded sparse matrices (see fig (3)) and are obtained from the 2D equation of the model in the isotropic case. In 4-connectivity the equation is

$$\begin{aligned} \tilde{V}_{(i,j)} &= V_{(i,j)} + \sum_{k=j-1,k\neq j}^{j+1} \frac{1}{\alpha}(V_{(i,j)} - V_{(i,k)}) \\ &+ \sum_{k=i-1,k\neq i}^{i+1} \frac{1}{\alpha}(V_{(i,j)} - V_{(k,j)}) \end{aligned} \quad (9)$$

where $\tilde{V}_{(i,j)}$ is the grey level of the original image, and $V_{(i,j)}$ is the value of the transformed pixel (i,j) .

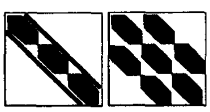

Figure 3: *Structure of* Γ^4_α *and* Γ^8_α

Writing the equation of this model for other kinds of neighbourhoods is straightforward.

5 Equivalent MSA filters

Here we give the expressions of three filters (1D and 2D isotropic, and 2D anisotropic) derived of the discrete operator Γ_α i.e. considering the generic equation of the system (4) : $(\alpha + 2)\, V_i - V_{i-1} - V_{i+1} = \alpha\, \tilde{V}_i$ (this is true only in $int(\Omega)$ but one can show that the boundary influence is negligible).

This recurrent equation leads naturally to a one dimensional linear filter expressed in the frequency domain by

$$\mathbf{H}^\alpha(\nu) = \frac{\alpha}{\alpha + 2\,(1 - \cos(2\,\pi\,\nu))} \quad (10)$$

(details of calculus are in [9]). In dimension 2 we obtain by tensorization $\mathbf{H}^\alpha_2(\nu_1,\nu_2) = \mathbf{H}^\alpha(\nu_1)\,\mathbf{H}^\alpha(\nu_2)$; and finally the third filter is obtained by $\tilde{\mathbf{H}}^\alpha_2(\nu_1,\nu_2) = \mathbf{H}^{\alpha_1}(\nu_1)\,\mathbf{H}^{\alpha_2}(\nu_2)$ with $\alpha_1 \neq \alpha_2$. This last filter allows us to favour the vertical or horizontal directions when $\alpha_1 \neq \alpha_2$ and leads to anisotropic treatments. The two first filters are lowpass when α is small and all-pass when α is very large (the link with (7) and (8) is easy).

6 Constrained scale change - The reconstruction problem

Up to now we have considered the case where the scale parameter is identical in all points of the network. This leads to an isotropic viewpoint. Furthermore the most interesting case is when α is not identical in all points, more specifically when α is given by a measure on the function to be studied i.e. $\alpha = \mu(f(x,y),x,y)$. As we can see in the scheme given in part 1, the goal is to make resolution changes without altering spatial location and altimetric information of important features. That is, certain points of the surface have to be fixed when the blurring is in progress. It is clear that we must choose the measures in accordance with the applications requested e.g. cartographers are not interested in the same surface measures than geologists who study stream networks. According to the matrix formulation that we use, it is very easy to consider different kinds of coupling between pixels and particularly assymetrical coupling, which leads to a modification of the diffusion, according to spatial directions. In this case, we do not respect the second Koenderink's principle and we adopt an anisotropic viewpoint. To demonstrate the feasibility of DEM reconstruction, with our model, we suppose that we are in a frame, where structures, like ridge lines and stream networks contain relevant information. To preserve the morphology of the reconstructed surface, we must adapt the scale parameter values around points belonging to these structures. The most natural way to do this is to fix points that belong to ridge lines and stream networks, and reconstruct the surface using only these points as "interpolation" nodes. The reconstruction process is given by the following scheme.

[1] Take $\mathcal{D}$ the set of all points that belong to ridge lines or stream networks (assumed to be given by an external process);

[2] Suppose that two points i and j are not only connected by one parameter α but by α_j^i in one direction and by α_i^j in the reverse direction. If we put $\alpha_j^i = \alpha_i^j$ we return at the original isotropic case and if we put $\alpha_j^i \neq \alpha_i^j$ the neighbourhood effect is not symmetrical and one can influence a point more or less, according to the value affected to the corresponding parameter.

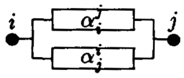

In the extreme case we want a point not to be influenced by others, but it should itself influence the others. For a point i , this is implemented by putting $\alpha_j^i = \infty$ and $\alpha_i^j = \alpha$: then the point i remains the same for all values of α , i.e. the location and altitude are preserved across the scales.

[3] When all parameters, between points that belong to $\mathcal{D}$ and the other points of the surface, are initialized, then we solve the linear system $\mathbf{\Gamma}_\alpha^4 V = \tilde{V}$ (e.g. in 4-connectivity) for different values of α , and we obtain a set of solutions, indexed by α .

To illustrate the use of this scheme, we give an example of DEM reconstruction. We choose to fix only ridge lines, stream networks and boundary points, all the others are left to 0 (no information). Figs (4)(a,b) show the 3D representation of the original DEM, and the points that have to be fixed to make the reconstruction. These points are obtained with the algorithm described in [8]. Figs (4)(c,d,e,f) show the reconstruction obtained for different numbers of iterations (we solve $\mathbf{\Gamma}_\alpha^4 V^{n+1} = V^n$ with $V^0 = \tilde{V}$). In figs (4)(g,h) we give the contour lines of the original and reconstructed DEM. These results are obtained by considering all surface points for the initialization of the algorithm. Some points are fixed (as in the first case) and the others are initialized with the original data. This leads to adopt a less brutal approach than in the first case where we have considered that no information is equivalent to 0. We can see that valleys are narrowed and the relief is more accentuated, but spatial morphology is relatively well conserved despite the smoothing.

This type of reconstruction cannot be considered as the ultimate one for all naturalist frameworks because, as we have seen, the measure employed to obtain α is context-dependent and it is very difficult to embed in it all the naturalist's knowledges.These examples only show the feasibility of such approach in a particular framework. In [9] we give also an example (isotropic case) with the test data given in [29].

Remark : Suppose we are in the 1D case. Fixing a point with $\alpha_j^i = \infty$ and $\alpha_i^j = \alpha$ is the same as putting a 1 on the diagonal element of the line i of $\mathbf{\Gamma}_\alpha$ and 0 elsewhere on this line. This naturally leads to an uncoupled system and this problem can be solved piecewise. However, discontinuities of the first derivative appear on frontier points of each subdomain, because the stationnary solution tends to be linear between two boundary points. One can show that to eliminate this "drawback" it is necessary to consider a model governed by a parabolic differential equation of degree four in space. We cannot develop this theoretical aspect due to space restrictions.

7 Conclusions

Techniques have been presented for doing scale changes of surfaces in the restricted case of DEM. The problem we had to solve was to make a preprocessing to the resolution change of DEM, constrained by morphological considerations.

We have studied a discrete evolution model (1D and 2D), based on electrical analogy, which conduces to a discrete multiscale operator. We have first studied the isotropic behaviour of this operator. Then we have discussed the reconstruction problem, and we have shown the ability of this model to take constraints upon pixel or region data into account.

To characterize the geometric transformation induced by this operator, we have shown that curves and surfaces are contracted relative to their average value. The contraction level is driven by a scale parameter which identifies the coupling of two pixels. Mathematically speaking, the multiscale operator reduces the norm of all signals by decreasing its curvature.

We have also shown that scale changes can be expressed in a probabilistic form : The 1D scaled operator is a transition probability matrix associated to a random Markov chain. And in a frequency form : The scaled operator is a filter (isotropic or anisotropic).

To test the ability of this operator in the framework of surface reconstruction, we have given some examples in which we have made the hypothesis that, 2D primitives, like ridge lines and stream networks contain relevant information and have to be fixed in the reconstruction process. The results are encouraging and show the adaptability of this model to various situations. Moreover it can be envisaged a parallel implementation, due to its discrete nature and its structure.

Acknowledgements

We would like to thanks N.Maman, J.M.Malé, P.Leymarie, S.Mathieu and B.Vasselle for their help in some parts of this study.

References

[1] E.H. Adelson, E. Simoncelli *Orthogonal Pyramid Transforms for Image Coding* SPIE Vol. 845 Visual Comm. & Im. Proc. II. 1987.

[2] J. Babaud, A.P. Witkin, M. Baudin, R.O. Duda *Uniquiness of the Gaussian Kernel for Scale-Space Filtering* IEEE Trans on PAMI - Vol 8 - No 1 - Jan 86.

[3] A. Blake et A. Zisserman *Visual Reconstruction*, MIT Press Cambridge MA 1987.

[4] R.M. Bolle , B.C. Vemuri *On Three-Dimensionnal Surface Reconstruction Methods* IEEE Trans on PAMI . Vol 13 . Jan 1991.

[5] T.E. Boult, J.R. Kender *Visual surface reconstruction using sparse depth data*, in Proc CVPR pp 68-76, 1986.

[6] P.Burt, E.H. Adelson *The Laplacian Pyramid as a Compact Image Code* IEEE Trans On Communications - Vol.Com-31, No.4, Apr 83.

[7] E.B. Davies *Heat Kernels And Spectral Theory* Cambridge Tracts in Mathematics No 92 - Cambridge University Press. 89.

[8] J. Fairfield, P. Leymarie *Drainage Networks From Grid Digital Elevation Models* Water Resources Research, Vol.27, No.5, Pages 709-717, May 91.

[9] F. Falzon, G. Giraudon, M. Berthod *Vers un Modèle pour l'Analyse Multiéchelle de Surface 3D* INRIA Report No 1639, 1992.

[10] C.A.J. Fletcher *Computational Techniques for Fluid Dynamics* Vol.I,II , Springer Series in Computational Physics, Springer Verlag.

[11] R. Franke, L.L. Schumaker *Bibliography of Multivariate Approximation*, in Topics in Mutilvariate Approximation, pp 275-335, 1987.

[12] J. Froment, J.M. Morel *Analyse Multiechelle, Vision Stereo et Ondelettes* in "Les Ondelettes en 1989" - Lectures Notes in Mathematics, Springer-Verlag , No 1438, pp 51-80.

[13] W.E.L. Grimson A Computational Study of the Human Early Visual System, MIT Press 1981.

[14] B.K.P. Horn *Robot Vision* The MIT Press McGraw-Hill Book company - 1986.

[15] R. Hummel *The Scale-Space Formulation of Pyramid Data Structures* Courant Institute - Tech report No 239 - Robotics Report No 77 - Aug 86.

[16] J.J. Koenderink *The Structure of Images* Biological Cybernetics , Springer-Verlag 1984.

[17] T. Lindeberg *Discrete Scale-Space Theory and the Scale-Space Primal Sketch* Ph-D dissertation May 91, TRITA-NA-P9108, Dept. Num. Anal. & Compt. Sci., Royal Inst. Tech. Sweden.

[18] A. Lumsdaine, J.L. Wyatt, I.M.Elfadel *Nonlinear Analog Networks for Image Smoothing and Segmentation* MIT Artificial Intelligence Laboratory. A.I. Memo No. 1280 - Jan 91.

[19] M. Mahowald, C. Mead *Une rétine en silicium* Pour la Science - No 165 - Jul 91.

[20] S.G. Mallat The Wavelet Representation IEEE Trans on PAMI. Vol 11. No 7 . Jul 89.

[21] J.L. Marroquin *Probabilistic Solution of Inverse Problems* Ph-D thesis, MIT, 1985.

[22] D. Marr, E. Hildreth *Theory of edge detection.* Proc. Roy. Soc. Lond. B207, 1980, 187-217.

[23] D. Mumford Do they model perception ? SPIE Vol. 1570 Geometric Methods in Computer Vision - 1991.

[24] K. Ottenberg *On Anisotropic Diffusion Process for Digital Image Processing* Robust Computer Vision. Förstner-Ruweidel Eds - WICHMAN , 2nd Int Workshop of Robust Computer Vision. Bonn, Mar 92.

[25] T. Poggio, V. Torre, C. Koch *Computational Vision and Regularization Theory* Nature Vol.317. 26 Sept 85.

[26] T. Poggio, V. Torre, C. Koch *An Analog Model of Computation For the Ill-Posed Problems of Early Vision* MIT - AI Laboratory, A.I.Memo 783, C.B.I.P Paper 002, May 84.

[27] L.L. Schumaker *Fitting Surfaces to scattered data*, In Approx. Th. II, Eds Lorentz, Chui, Schumaker, pp 203-268, Academic Press, 1976.

[28] S.S. Sinha, B.G. Schunck *Surface Approximation Using Weighted Splines*, in Proc CVPR Hawai Jun 91.

[29] R. Szeliski *Fast surface interpolation using hierarchical basis function*, IEEE PAMI, Vol 12(6), pp 513-528, Jun 90.

[30] D. Terzopoulos *The Computation of visible-surface representations* IEEE Trans on PAMI Vol 10(4) pp 417-438, 1988.

[31] D. Terzopoulos, M.Vasilescu *Sampling and Reconstruction with Adaptative Meshes*, in Proc CVPR Hawai 91.

[32] A.P. Witkin *Scale-Space Filtering* Proc. of IJCAI, 1019-1022, Karlsruhe 1983.

[33] A.L. Yuille, A. Poggio *Scaling Theorems for Zero Crossings* IEEE Trans on PAMI, Vol. PAMI-8, 1, Jan 86.

[34] Yong-Jian Zheng *Inductive Inference and Inverse Problems in Computer Vision* Robust Computer Vision. Förstner-Ruweidel Eds - WICHMAN , 2nd Int Workshop of Robust Computer Vision. Bonn, Mar 92.

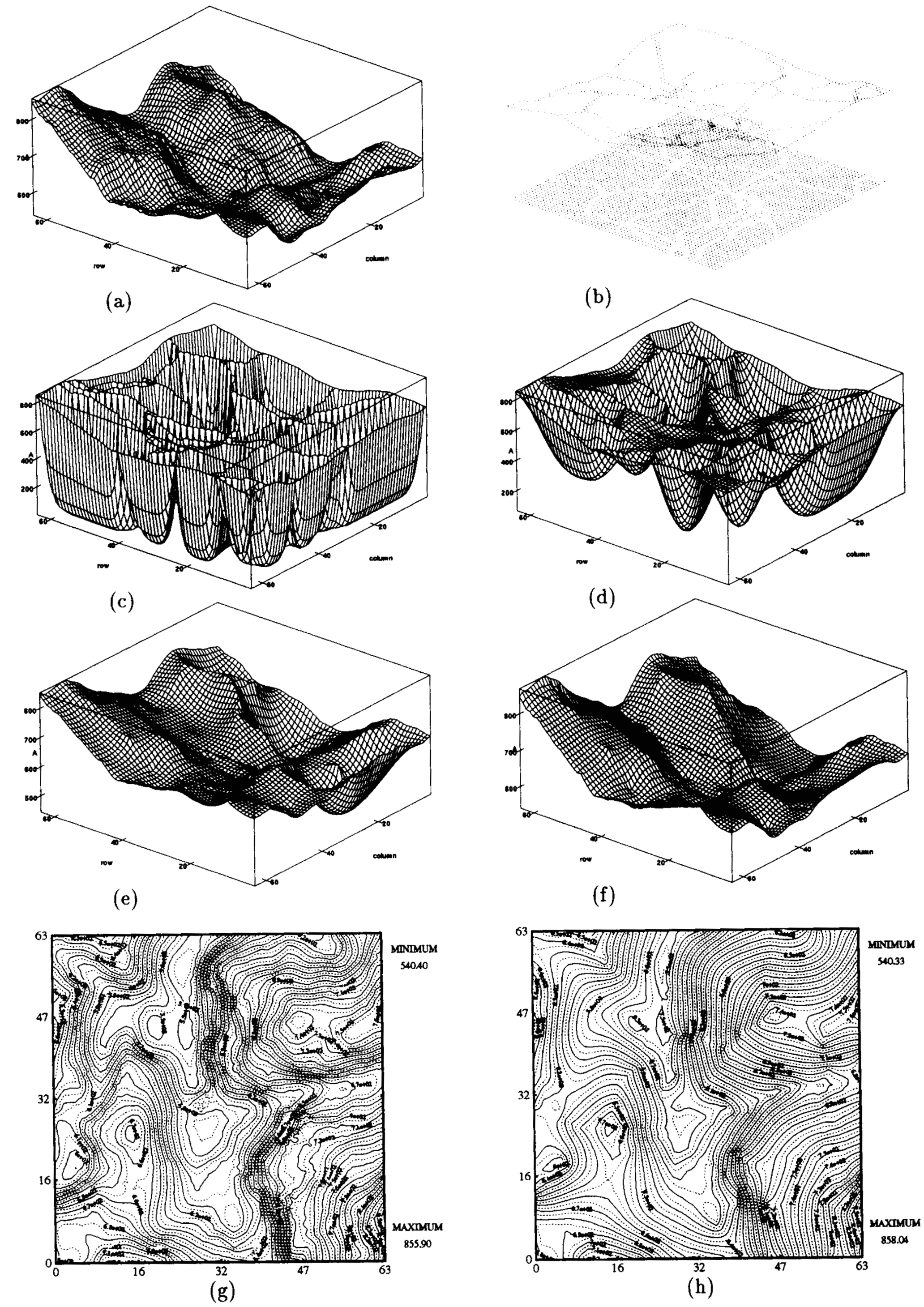

Figure 4: **(a)** *Original DEM;* **(b)** *Ridge line, stream network and boundary points (* 814 *points* $\sim$ 20% *of the original DEM points);* **(c)** 2 *iterations;* **(d)** 20 *iterations;* **(e)** 80 *iterations;* **(f)** 150 *iterations. (we have taken* $\alpha = 2$ *).* **(g)** *Contour lines of the DEM given in (a);* **(h)** *Contour lines of the reconstructed DEM.*